Original Article

A Monte Carlo study on quantifying the amount of dose reduction by shielding the superficial organs of an Iranian 11-year-old boy

Parisa Akhlaghi, Elie Hoseinian-Azghadi[1], Hashem Miri-Hakimabad[1], Laleh Rafat-Motavalli[1]

Department of Medical Physics, Faculty of Medicine, Tabriz University of Medical Sciences, Tabriz, [1]Department of Physics, Faculty of Science, Ferdowsi University of Mashhad, Mashhad, Iran

Received on: 14-05-2016 **Review completed on:** 22-08-2016 **Accepted on:** 22-08-2016

ABSTRACT

A method for minimizing organ dose during computed tomography examinations is the use of shielding to protect superficial organs. There are some scientific reports that usage of shielding technique reduces the surface dose to patients with no appreciable loss in diagnostic quality. Therefore, in this Monte Carlo study based on the phantom of a 11-year-old Iranian boy, the effect of using an optimized shield on dose reduction to body organs was quantified. Based on the impact of shield on image quality, lead shields with thicknesses of 0.2 and 0.4 mm were considered for organs exposed directly and indirectly in the scan range, respectively. The results showed that there is 50%–62% reduction in amounts of dose for organs located fully or partly in the scan range at different tube voltages and modeling the true location of all organs in human anatomy, especially the ones located at the border of the scan, range affects the results up to 49%.

Key words: Computed tomography examinations; dose reduction; Iranian voxel phantom; lead shield

Introduction

The principal long-term disadvantage of computed tomography (CT) is the radiation exposure. The risk of cancer increases linearly with increasing dose until extensive cell killing takes place at very high exposures. The cancer risk depends on both sex and age, with higher risks for females and for those exposed at younger ages.[1] Improvements in CT technology (e.g., detector efficiency, geometry efficiency, tube current modulation, and reconstruction algorithms) have decreased patient doses significantly. Beginning in the 1990s, remarkable efforts have been made to lower the dose to the pediatric population.[2] By changing the CT parameters based on the patient's weight or age, the dose is reduced significantly. However, the radiation dose should only be reduced under the condition that the diagnostic image quality is not sacrificed to ensure appropriate diagnosis.

A long accepted method of dose minimization during radiographic examinations is the use of shielding to protect superficial organs.[3,4] These shields allow meaningful reduction in dose to superficial organs through the absorption of lower energy dose contributing photons, while they are not degrading image quality. Applying this method was started in the early 2000s. Fricke *et al*. studied the amount of dose reduction using bismuth for shielding breast in multidetector CT (MDCT) of the chest and abdomen in female pediatric patients. The results indicated that shield enabled a 6.7% decrease in the radiation dose to the lungs and a 29% decrease to the breast with no appreciable loss in diagnostic quality.[5] Coursey

Address for correspondence:
Dr. Parisa Akhlaghi,
Department of Medical Physics, Faculty of Medicine, Tabriz University of Medical Sciences, Golgasht Ave., Tabriz, Iran.
E-mail: parissa_akhlaghi@yahoo.com

Access this article online	
Quick Response Code:	Website: www.jmp.org.in
	DOI: 10.4103/0971-6203.195189

How to cite this article: Akhlaghi P, Hoseinian-Azghadi E, Miri-Hakimabad H, Rafat-Motavalli L. A Monte Carlo study on quantifying the amount of dose reduction by shielding the superficial organs of an Iranian 11-year-old boy. J Med Phys 2016;41:246-53.

et al. assessed the effect of bismuth breast shields on the radiation dose during pediatric chest 16-MDCT. Using this shield with a tube current of 65 mA, the breast dose was reduced by 26%.[6] In 2007, eye absorbed dose (lens and orbit) was measured during pediatric cranial MDCT with and without bismuth shielding. The average dose reduction in eyes was 42% at 120 kVp.[7] In 2011, eye and thyroid doses were assessed using a bismuth shield in Slovakia. The best reduction in the eye dose due to the use of bismuth shields was within the range of 56–65%, and it was 25% for thyroid. Applying an eye shield, some artifacts were observed but the decrease in image quality was not unsatisfactory.[8] In our previous feasibility study, we investigated the effects of using our designed bismuth and lead shields with different thicknesses (0.1–0.5 mm) on dose reduction and image quality in pediatric CT imaging. As known, for external radiation, the depth below the surface is a parameter that significantly influences the dose. Therefore, thickness of the shield is a determinant parameter that indicates how much each point of an organ or tissue is shielded from radiation impinging from X-ray source.[9] The preliminary results showed that if superficial organs are not the target of CT imaging, lead shields cannot interfere with the interpretation of the image and as the organ's shield is excluded from the imaging field, the presence of shield is inconsequential in terms of image quality. Given the results and more availability of lead, it was proposed as the beneficial shield for protecting the superficial organs.[10] There are many differences between the anatomies of simplified model of Oak Ridge National Laboratory (ORNL) phantoms and detailed voxel-based phantoms. Since anatomy and body composition affect the resulting radiation dose, the differences between the dosimetric data for different individuals should be evaluated. This could help the user to decide, based on more accurate data, whether a protective shield is needed for children in various scans. Moreover, a vast database could provide more precise estimations of cancer risk.[9]

The emphasis of the previous study was on finding a suitable shield with less impact on image quality. In this regard, the effects of different shields on the X-ray spectrum were investigated, and the selection of appropriate shield was based on studying the physical properties and the possibility of Compton and photoelectric interactions with applying different shields. Dose reduction with simple anatomical models was also studied in the process, in order to make a proper decision. To make these shields commercially available, the results should be comprehensive and more accurate. Therefore, in this study, we took a step forward to investigate the effects of recommended shield on dose reduction to superficial organs of a real anatomical model of a child, who is close to reference 11-year-old boy in terms of height and weight.

Considering the benefits of using shield, especially for organs located in the scan range, which are not the target of imaging, the purpose of this study is to determine the amount of dose reduction for an Iranian 11-year-old voxel phantom by applying lead shield by Monte Carlo simulation. Hence, we wanted to investigate the level of effectiveness of exact modeling of the organs' location and shape on the results of dose reduction.

In external radiations, the absorbed doses of organs depend on their distances from the body surface.[9] On the other hand, various organs are not local in one place, so the distances of their voxels from the surface vary significantly. Therefore, the amount of absorbed dose, which represents the averaged value of dose for all voxels of an organ, cannot determine the dose delivered to each voxel. Therefore, a dose map, which contains dose value in each voxel, is needed. As far as we know, there is no report on the dose distribution of organs located under the shield, and this issue will be discussed in this research.

Materials and Methods

Iranian 11-year-old male phantom

Since anatomy and body compositions affect the resulting radiation dose, in the present study, we estimated the dose values for a reference Iranian 11-year-old male phantom developed in our institute. The anatomical model of this voxel phantom was developed based on the image sets of whole-body scan of an Iranian 11-year-old male volunteer, who had weight of 34.63 kg and height of 147 cm.

Magnetic resonance imaging (MRI) was used to image the volunteer (instead of CT), based on the ethical considerations (absence of ionizing radiation, – especially important for children) and the improved soft tissue contrast of MRI. The volunteer was scanned on a 1.5 T Siemens Magnetom Avanto whole-body scanner at the radiological department of Ghaem Hospital, Mashhad, Iran. The entire scanning time, including breaks for the volunteer, was ~3 h.

A radiologist, who had expertise in pediatric anatomy, identified the organs and tissues in the MRI images. Based on his identification, manual segmentation was performed using 3D-DOCTOR™ (Able Software Corp., Lexington, MA, USA), a three-dimensional (3D) modeling and image-processing software package. About 104 different tissues and organs were identified and segmented for the model. All the organ models were imported to Rhinoceros (McNeel, Seattle, WA, USA), and they were oriented and their locations were adjusted. To incorporate the models into Monte Carlo code, all organs were voxelized using a voxelizer developed by our research group in FORTRAN code. The voxel resolution was 0.15 cm × 0.15 cm × 0.3 cm, and the voxel array size was 300 × 170 × 490.[9] It should be mentioned that this phantom is anatomically close to the reference values

reported by International Commission on Radiological Protection (ICRP) publication 89.[11] Therefore, the density and the elemental composition of organs and tissues of reference 11-year-old male voxel phantom developed at University of Florida (UF) were attributed to those of the Iranian phantom. Note that the anatomical and physiological data of UF phantom is closely aligned to those of ICRP publication 89.[12,13] Figure 1 represents the model of Iranian 11-year-old male.

Monte Carlo dose estimation method

To obtain organ dose in a human body, two different approaches are possible: Experimental procedures and Monte Carlo simulation. It was reported that Monte Carlo simulation is the most reliable way to obtain accurate values of organ dose,[14,15] because the pediatric bodies lying on a CT table and X-ray beam are fully simulated so that with an appropriate simulation model, the results are acceptable.

Some Monte Carlo programs using MCNP,[15-18] PENELOPE,[19] and EGSnrc[20,21] were developed which simulate the dose inside the computational models of the human body. Most recent studies on pediatric CT simulations were performed by MCNP. Therefore, for comparability of our results with those reported in recent literature with the same scanner, in this study, MCNP4C, developed by Los Alamos National Laboratory, was used for photon transport. The photon transport model creates electrons but assumes that they travel in the direction of the primary photon and that the electron energy is deposited at the photon interaction site, creating a condition of charged particle equilibrium (CPE). In other words, CPE exists for a volume if each charged particle of a given type and energy leaving this volume is replaced by an identical particle of the same energy entering. Under conditions of CPE, collision kerma, which is the sum of the initial kinetic energies of all the charged particles liberated by ionizing radiation, is valid to be equal or very approximate to absorbed dose.[22] Therefore, absorbed dose was approximated by collision kerma and was recorded using track length estimate of photon energy deposition tally (F6:p). The simulations provide energy deposition (MeV) per unit mass (g), per emitted particle. Considering that the unit of absorbed dose is Gy (J/kg), the output of the programs should be multiplied by 1.6×10^{-10}.[23]

For determination of the amount of dose reduction achievable by shielding the superficial organs, the absorbed doses for organs, which were irradiated directly (eye lenses in head scan) or were mainly exposed by scattered radiation (thyroid in chest scan and testes in abdomen-pelvis scan) were calculated without and with lead shields. In addition to graphically displaying dose map in the model, F6 tally was used and dose was recorded in each voxel.[24] Using this approach, the variations of dose with position in Iranian 11-year-old phantom without and with lead shield were determined in different tube voltages. To compare the absorbed doses and dose distributions, the same parameters were considered for both steps. A total of 10^9 photons were simulated to obtain reasonable relative errors (<2%) for major organs and tissues located in the scan coverage. Errors were obviously higher for the tissues located outside of the scan region (up to 5%). Table 1 includes the parameters considered in the simulations.

Computed tomography scanner modeling

The scanner of Siemens Somatom Sensation 16 (Siemens Medical Systems, Germany) was simulated within the code. The CT scanner had a beam originating from the focal spot with an angle of 52°, a target material made of tungsten and a focal spot-to-axis distance of 57 cm. The information about X-ray spectra and scanner's filter was provided by the manufacturer. As the absorbed doses to internal organs are known to vary inversely with detector pitch,[18] single detector pitch of 1 was selected for all the simulations.

There are at least three ways to define the specific shape of the fan beam.[16,22,25] One way is to use many discrete

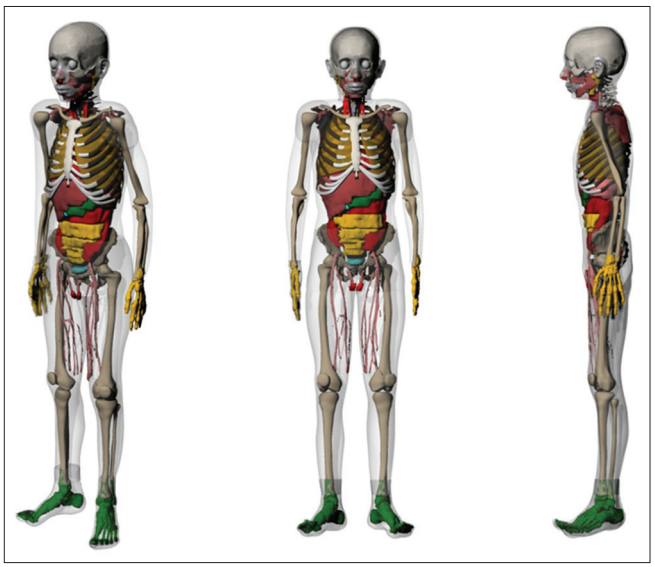

Figure 1: Different views of an Iranian 11-year-old male phantom

Table 1: The scan parameters considered in the simulations

Tube voltage (kVp)	*Collimation (cm)*	*Pitch*	*Scan coverage*		
			Head	*Chest*	*Abdomen-pelvis*
80, 100 and 120	1	1	From top of the head to the 2nd cervical vertebra	From the clavicles to the middle of the liver	From the top of liver to the midfemoral head

point sources, each consisting of many individual pencil beams, which simulate the fan-shaped beam.[16]

To model CT scanner and fan beam, the method described by Khursheed *et al*. was applied. As stated by them, 18 sources were sufficient to approximate the continuous circular movement of the source, without significantly affecting the calculated organ doses. Therefore, CT imaging was simulated by exposing a series of contiguous transverse slices of 1 cm thickness to emit X-rays from 18 sources lying on a circle with a radius equal to focal spot-to-axis distance around the phantom. Photons are emitted normal to each line source, but unconstrained otherwise, i.e., over 360°. The photons that are tracked through the phantom essentially arise from a fan-shaped beam from each source that is perfectly collimated to the phantom and has parallel sides 1 cm apart.[16]

The accuracy of the simulation was verified by comparing the measured CT dose index (CTDI) values with those obtained by simulation. For this purpose, CTDI data were calculated for head CTDI phantom with diameters of 16 cm, and were compared with CTDI values measured by Lee *et al*.[15,17] under the same radiation exposure conditions. Moreover, the peripheral CTDI value at 12 o'clock was measured, and it was then compared with the result of the simulation. A 10 cm pencil-shaped Radcal® ion chamber model 10 × 5-3CT (Radcal Corporation, Monrovia, CA, USA) and a Radcal 9015 dosimeter (Radcal Corporation, Monrovia, CA, USA) were used to determine the CTDI values.[26] To perform the comparison, the CTDI head phantom was modeled as a cylinder having a diameter of 16 cm, with a length of 15 cm. The material composition of CTDI phantom was simulated as polymethylmethacrylate with a density of 1.19 g/cm^3. The ion chamber was modeled as three 10 cm long concentric cylinders. The innermost cylinder, with a diameter of 0.67 cm, defined the active air volume. The second cylinder, with a diameter of 1.02 cm, defined the chamber wall, which was C552 air-equivalent material with a density of 1.76 g/cm^3. The third cylinder, with a diameter of 1.37 cm, defined a build-up cap, which was modeled as polyacetal plastic with a density of 1.43 g/cm^3.[9] Figure 2 displays the CTDI phantom and the ion chamber used for model validation. Moreover, in Figure 3, a plot from the simulated CTDI phantom and ion chamber is illustrated.

Placing appropriate in-plane shield

At general diagnostic imaging energies in soft tissues and bone, a large fraction of the attenuation occurs by Compton scatter rather than by photoelectric absorption, chiefly because of the low atomic number of the tissues. X-ray scatter reduces subject contrast by adding background signals that are not representative of the anatomy. But, in the photoelectric absorption, there are no additional nonprimary photons to degrade the image. It could be said that image contrast decreases when higher X-ray energies are used in the imaging process.[27] Therefore, with an optimized shield, higher and lower parts of spectrum will be removed while the characteristic peaks of the spectra will not. In this regard, in the previous study, we investigated the effects of different thicknesses (0.1–0.5 mm) of bismuth and lead on the X-ray spectra. It was observed that the high thickness of shield has more destructive effect on image quality. This is due to the fact that a shield affects the whole spectrum, not only does it remove the lower energy parts, but it also increases the relative number of Compton scatter in higher energies. For a detailed study, the effects of applying lead and bismuth with thicknesses of 0.1–0.5 mm on dose reduction of ORNL stylized phantoms were also investigated. For all organs, dose reduction was higher for lead shield. Moreover, there was an exponential relationship between absorbed doses and the thickness of shield, implying that there is an optimal thickness beyond which no significant reduction in dose can be achieved with further increase in shield thickness. Given the results of dose reduction, X-ray spectra analysis and the weight of protective shield, a lead shield with thickness of 0.2 mm was selected and its effect on image quality was experimentally studied using CT calibration phantom.[10] Based on these observations, a shield with thickness of 0.2 mm was suggested for shielding the superficial organs exposed directly to the radiation, which is the optimized thickness to remove the lower energies. On the other hand, the destructive effect of thicker layer on the image quality is not an issue for organs located out of the scan range. Hence, the only limitation is the weight of shield, which should be light to neither disturb the patient's comfort during a CT examination nor interfere with the patient's respiration. Therefore, for organs located out of the scan range, a shield with thickness of 0.4 mm was suggested for different tube voltages.

To place the appropriate shield on the superficial organs of Iranian voxel phantom, our designed lead shields with

Figure 2: Computed tomography dose index phantom and an ion chamber placed in position of 12 o'clock

mentioned thicknesses were modeled on the eyes, thyroid, and testes of Iranian 11-year-old boy, using 3D-DOCTOR. Lead shield was considered as protective shield to cover the anterior surface of the phantom, and it did not exceed the width of the anterior surface. Then, to incorporate the new geometries into MCNP4C, the whole model was voxelized applying the mentioned FORTRAN code developed in Ferdowsi University of Mashhad.[9,28]

Results

Benchmarking

Four different point doses (central dose and doses at 12, 3, and 6 o'clock positions) were determined within the head phantom by using the ion chamber with the collimation of 10 mm under the three tube potentials of 80, 100, and 120 kVp. The measured and simulated values of peripheral CTDI at 12 o'clock at tube voltage of 80 kVp, were 7.25 and 6.81, respectively. The weighted CTDI ($CTDI_w$), which is defined as the summation of one-third of $CTDI_{center}$ and two-thirds of $CTDI_{periphery}$, was 6.20, 11.60, and 16.20 mGy, for CTDI head phantom at tube voltages of 80, 100, and 120 kVp, respectively.[9,28] The simulated doses of this study agreed with the measured ones with maximum error of almost 9% for all tube potentials. These results were comparable with those given in other published studies.[15,17] Table 2 contains the results obtained for $CTDI_w$ in comparison with other studies.

Lead shield on superficial organs

In Figure 4, the lead shield with mentioned thickness (0.2 mm) is modeled on the eyes of voxel phantom. In the figure, the shield covering the eyes is in red.

Dose estimations

Table 3 displays eyes, thyroid, and testes doses in mGy/mAs at tube voltages of 80, 100, and 120 kVp without and with lead shield. From the table, it is obvious that these small thicknesses of shield reduce the received doses. For instance, at tube voltage of 80 kVp, the amounts of dose reductions of eyes (using a lead shield with thickness of 0.2 mm), thyroid (using a lead shield with thickness of 0.4 mm), and testes (same shield as thyroid) are 62%, 18%, and 58%, respectively. On the other hand, it is observed that increasing the voltage decreases the dose reduction effects achievable by shield.

Moreover, dose distribution maps of 11-year-old phantom without and with shield at Z = 135.75 cm at tube voltage of 80 kVp are illustrated in Figure 5. According to the figure, not only was the dose reduced in eyes, but the surrounding tissues also received less amounts of dose. The maximum reduction (e.g., almost 60% for eyes) was observed in the anterior surface (directly below the shield) and the minimum reduction was almost 5% for areas located far from the shield, for which there is greater contribution of

Table 2: The weighted computed tomography dose index values for head phantom in different tube potentials obtained in this study in comparison with other investigations (errors were <2%)

Tube voltage (kVp)	*$CTDI_w$ (mGy)*	
	This study	*Lee et al. study*
80	6.2	6.1
100	11.6	10.8
120	16.2	15

$CTDI_w$: Weighted computed tomography dose index

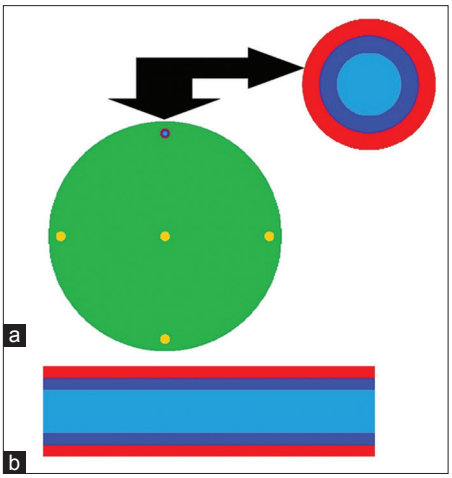

Figure 3: MCNP plot of simulated (a) computed tomography dose index phantom (axial view), and (b) ion chamber (transversal view). Ion chamber was located at 12 o'clock position in computed tomography dose index phantom

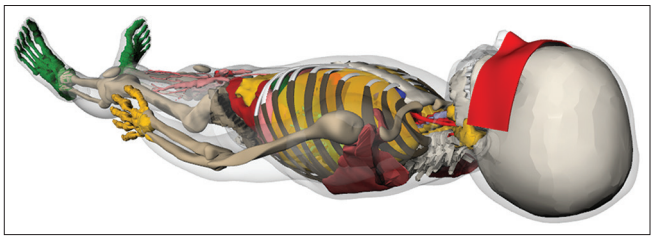

Figure 4: Lead shield covers the eyes of Iranian boy voxel phantom

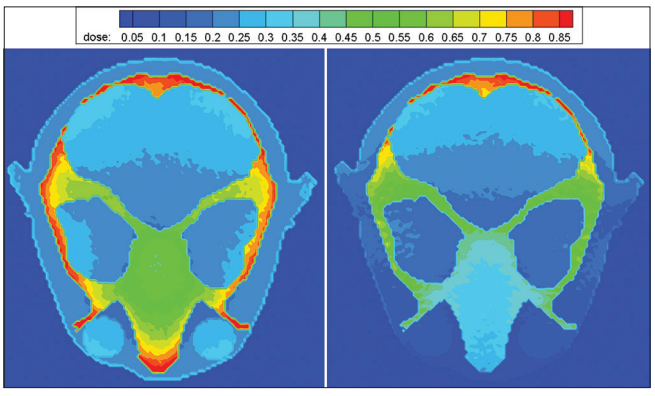

Figure 5: Dose distribution map in mGy per mAs without (left) and with (right) lead shield with thickness of 0.2 mm at 80 kVp

Table 3: The amounts of eyes, thyroid, and testes doses without and with lead shield in mGy/mAs for different tube voltages

Tube voltage (kVp)	*Eyes dose (head scan)*		*Thyroid dose (chest scan)*		*Testes dose (abdomen-pelvis scan)*	
	Without shield	*With shield*	*Without shield*	*With shield*	*Without shield*	*With shield*
80	2.46E-2	9.46E-3	6.94E-3	5.67E-3	2.01E-2	8.47E-3
100	5.12E-2	2.36E-2	1.53E-2	1.29E-2	4.13E-2	1.94E-2
120	8.64E-2	4.27E-2	2.62E-2	2.24E-2	6.89E-2	3.39E-2

X-ray beams from the non-shielded aspect of the phantom compared to that from the shielded aspect.

Discussion

Given the dramatic rise in its use worldwide, radiation dose remains a concern within CT.[29] Despite the introduction of newer technologies, there has been a reported increase in average CT dose with the advent of multidetector technology;[30] therefore, any efforts to reduce dose to the sensitive organs will be of particular benefit in lowering the risks of CT examinations.[31]

One of the common techniques for radiation dose management is automatic exposure control (AEC),[6,32] which adjusts scanner output based on the patient attenuation to deliver a user-specified level of image noise. In this technique, system characteristics, patient anatomy, and user-specified requirements for image quality are determined before scan. A user assigns the image quality requirements (noise or contrast to noise ratio), and the CT system determines the right tube current–time product. Sometimes, it is quite difficult to achieve agreement on the image quality requirement for the various CT examination types and patient age groups. In defining the required image quality, the user needs to remember that pretty pictures are not needed for all diagnostic tasks, but rather a choice can be made between low noise and a low dose, depending on the diagnostic task. The CT system will then adjust the tube current during the gantry rotation, during movement along the *z*-axis, or during movement in all 3D, according to the patient's body and the user's image quality requirements.[33] According to the American Association of Physicists in Medicine statement, users can change AEC parameters to more aggressively decrease the tube current. However, it should be noted that since AEC systems on CT scanners can be complex and involve adjustments of several parameters, they are urged to consult with a medical physicist and/or applications specialist when making changes to the AEC parameters.[34] In some countries, AEC systems are not implemented in all CT scanners and are not commonly used in radiology departments.

As stated before, in diagnostic imaging, Compton scattering reduces subject contrast, while in the photoelectric absorption, there are no additional nonprimary photons to degrade the image.[27] In addition, photons with lower energies are absorbed in the superficial tissues of the body and do not contribute in image construction and just increase received doses, especially in sensitive organs such as thyroid, eyes, and gonads. Applying a shield optimizes the X-ray spectra by removing the higher and lower energy parts of the spectrum.[10]

The additional filters of X-ray tube harden the radiation beam before it reaches the patient by absorbing soft X-ray photons so that a more homogenous beam is utilized for imaging. As a consequence of prefiltering, both beam hardening effect and patient's absorbed dose are intrinsically reduced; however, as a compromise, statistical noise is increased, which in turn impairs the image quality due to total reduction beam intensity per mAs as experienced by the detectors.[35] As known, noise may affect the diagnostic ability in low-contrast regions, so acceptable levels of noise and image quality within CT images is an important point, which can be different even within one scan range, depending on the anatomy included. Alternatively, the use of superficial shielding can offer a solution to this predicament, as shielding is applied only to body surface and dose can be maintained at optimal levels outside of the region of interest.[36]

It was reported that good radiographic technique includes the standard use of lead or equivalent shielding of child's body in the immediate proximity of the diagnostic field and if shields are placed appropriately with enough distance to minimize the subjacent artifact, they can be used to protect superficial organs from direct or scattered radiation.[37] Therefore, in this study, lead shield was selected for protecting superficial organs, because, eyes, thyroid, and testes are not usually the target organs during CT imaging, and they receive radiation dose as a byproduct of their anatomical locations. These scales of absorbed doses reinforce the need for using any technique, which reduces doses to these radiosensitive tissues (in compliance with the ALARA principle) and does not affect image quality.[36]

Considering our previous publication, the optimum thickness of shield is the one with the minimum effect on the image quality. This means that changes in Hounsfield unit, image noise, and artifacts due to applying this optimized

shield do not interfere with the image interpretation. Therefore, lead shields with thicknesses of 0.2 mm and 0.4 mm were placed on the organs located in (e.g., eye) and out (e.g., thyroid) of the scan range, respectively.[10]

From the results, it is obvious that the amount of dose reduction for organs exposed to scattered radiation (up to 18%) is not as significant as organs exposed directly in the scan range (up to 62%). This is due to the fact that for organs located completely out of the scan range (thyroid in chest scan), internal scattering of exposed radiation in the body has the most contribution (almost 98%) in the amount of absorbed doses,[10] so less amounts of radiation are received by the organ through the air. Besides, a superficial shield protects organs from external radiation; thus shielding these organs has less effect on the amount of dose reduction.

In addition, it is observed that the amount of dose reduction in testes is more than that in thyroid. This is quite in contrast to the results obtained for stylized phantoms of ORNL, for which the thyroid dose reduction is higher. This discrepancy is due to the differences that exist in the anatomies of voxel and stylized phantoms. As stated, internal scattering has the most contribution (almost 98%) in the absorbed doses of organs located out of the scan range,[10] so their distance from scan range plays an important role in the level of dose.

In voxel phantom, the distance of thyroid relative to the chest scan region is more than that in ORNL phantom, whereas his testes are closer to the scan region so that part of them is exposed directly in the abdomen-pelvis scan field. Given the outcomes, the importance of modeling true location of all organs in human anatomy is explicit.[38] In the study based on stylized phantom, the testes dose reduction was 9%, whereas in this study, this value rises up to 58%. Because of these more accurate results, no one should ignore placing lead shield on testes in abdomen-pelvis scan.

On the other hand, from Figure 5, dose reduction is more significant directly below the shield, due to increased attenuation of the incident X-ray beam at the shielded surface compared to the opposite nonshielded aspect of the head. However, less pronounced but definite decrease exists in the doses of further voxels, which could be explained by the greater contribution of X-ray beams from the nonshielded aspect of the phantom compared to that from the shielded aspect.

Conclusion

In this study, the importance of using lead shield on superficial organs of an Iranian 11-year-old phantom for the purpose of dose reduction was investigated. Therefore, the absorbed doses of eye lenses, thyroid, and testes as well as dose distribution were estimated for Iranian 11-year-old phantom undergoing CT examinations without and with shield at tube potentials of 80, 100, and 120 kVp. The dose reductions were 62%, 18%, and 58%, for eyes, thyroid, and testes, respectively, at 80 kVp. In addition, based on dose distribution, a definite decrease in doses for other organs located in the scan range was observed. It could be said that shielding the superficial organs can play an important role in dose optimization during CT scanning.

Acknowledgment

The authors would like to acknowledge Dr. Karl Stierstorfer for providing the X-ray spectra of the Siemens Somatom Sensation 16 scanner.

Financial support and sponsorship

Nil.

Conflicts of interest

There are no conflicts of interest.

References

1. Committee on the Biological Effects of Ionizing Radiation. Health risks from exposure to low levels of ionizing radiation. BEIR VII, Phase 2. Washington: The National Academies Press; 2005. p. 21-172.
2. International Commission on Radiological Protection (ICRP). Managing patient dose in computed tomography. ICRP publication 87. Ann ICRP 2000;30:1-45.
3. Hopper KD, King SH, Lobell ME, TenHave TR, Weaver JS. The breast: In-plane X-ray protection during diagnostic thoracic CT – Shielding with bismuth radioprotective garments. Radiology 1997;205:853-8.
4. Parker MS, Kelleher NM, Hoots JA, Chung JK, Fatouros PP, Benedict SH. Absorbed radiation dose of the female breast during diagnostic multidetector chest CT and dose reduction with a tungsten-antimony composite breast shield: Preliminary results. Clin Radiol 2008;63:278-88.
5. Fricke BL, Donnelly LF, Frush DP, Yoshizumi T, Varchena V, Poe SA, *et al.* In-plane bismuth breast shields for pediatric CT: Effects on radiation dose and image quality using experimental and clinical data. AJR Am J Roentgenol 2003;180:407-11.
6. Coursey C, Frush DP, Yoshizumi T, Toncheva G, Nguyen G, Greenberg SB. Pediatric chest MDCT using tube current modulation: Effect on radiation dose with breast shielding. AJR Am J Roentgenol 2008;190:W54-61.
7. Mukundan S Jr., Wang PI, Frush DP, Yoshizumi T, Marcus J, Kloeblen E, *et al.* MOSFET dosimetry for radiation dose assessment of bismuth shielding of the eye in children. AJR Am J Roentgenol 2007;188:1648-50.
8. Gbelcová L, Nikodemová D, Horváthová M. Dose reduction using bismuth shielding during paediatric CT examinations in Slovakia. Radiat Prot Dosimetry 2011;147:160-3.
9. Akhlaghi P, Miri-Hakimabad H, Rafat-Motavalli L. Dose estimations for Iranian 11-year-old pediatric phantoms undergoing computed tomography examinations. J Radiat Res 2015;56:646-55.
10. Akhlaghi P, Miri-Hakimabad H, Rafat-Motavalli L. Effects of shielding the radiosensitive superficial organs of ORNL pediatric phantoms on dose reduction in computed tomography. J Med Phys 2014;39:238-46.
11. International Commission on Radiological Protection (ICRP). Basic anatomical and physiological data for use in radiological protection:

Reference values. A report of age- and gender-related differences in the anatomical and physiological characteristics of reference individuals. ICRP Publication 89. Ann ICRP 2002;32:5-265.
12. Lee C. Development of the voxel computational phantoms of pediatric patients and their application to organ dose assessment. PhD Thesis. The University of Florida; 2006.
13. Lee C, Williams JL, Lee C, Bolch WE. The UF series of tomographic computational phantoms of pediatric patients. Med Phys 2005;32:3537-48.
14. DeMarco JJ, Cagnon CH, Cody DD, Stevens DM, McCollough CH, O'Daniel J, *et al*. A Monte Carlo based method to estimate radiation dose from multidetector CT (MDCT): Cylindrical and anthropomorphic phantoms. Phys Med Biol 2005;50:3989-4004.
15. Lee C, Kim KP, Long D, Fisher R, Tien C, Simon SL, *et al*. Organ doses for reference adult male and female undergoing computed tomography estimated by Monte Carlo simulations. Med Phys 2011;38:1196-206.
16. Khursheed A, Hillier MC, Shrimpton PC, Wall BF. Influence of patient age on normalized effective doses calculated for CT examinations. Br J Radiol 2002;75:819-30.
17. Lee C, Kim KP, Long DJ, Bolch WE. Organ doses for reference pediatric and adolescent patients undergoing computed tomography estimated by Monte Carlo simulation. Med Phys 2012;39:2129-46.
18. Lee C, Lee C, Staton RJ, Hintenlang DE, Arreola MM, Williams JL, *et al*. Organ and effective doses in pediatric patients undergoing helical multislice computed tomography examination. Med Phys 2007;34:1858-73.
19. Li X, Samei E, Segars WP, Sturgeon GM, Colsher JG, Toncheva G, *et al*. Patient-specific radiation dose and cancer risk estimation in CT: Part I. development and validation of a Monte Carlo program. Med Phys 2011;38:397-407.
20. Bazalova M, Verhaegen F. Monte Carlo simulation of a computed tomography X-ray tube. Phys Med Biol 2007;52:5945-55.
21. Oono T, Araki F, Tsuduki S, Kawasaki K. Monte Carlo calculation of patient organ doses from computed tomography. Radiol Phys Technol 2014;7:176-82.
22. Gu J, Bednarz B, Xu XG, Jiang SB. Assessment of patient organ doses and effective doses using the VIP-Man adult male phantom for selected cone-beam CT imaging procedures during image guided radiation therapy. Radiat Prot Dosimetry 2008;131:431-43.
23. Briesmeister JF. MCNP™–A General Monte Carlo N–Particle Transport Code, Version 4C, LA–13709–M. Los Alamos National Laboratory, Los Alamos, USA; 2000.
24. Akhlaghi P, Miri Hakimabad H, Rafat Motavalli L. Determination of tissue equivalent materials of a physical 8-year-old phantom for use in computed tomography. Radiol Phys Chem 2015;112:169-76.
25. Gu J, Bednarz B, Caracappa PF, Xu XG. The development, validation and application of a multi-detector CT (MDCT) scanner model for assessing organ doses to the pregnant patient and the fetus using Monte Carlo simulations. Phys Med Biol 2009;54:2699-717.
26. Radcal Corporation. Available from: http://www.radcal.com/10x5-3ct. [Last accessed on 2016 May 07].
27. Bushberg JT, Siebert JA, Leidholdt EM, Boone JM. Computed tomography. In: The essential physics of medical imaging Vol. 1, Philadelphia: Lippincott Williams and Wilkins; 2002. p. 327-72.
28. Akhlaghi P, Hakimabad HM, Motavalli LR. Evaluation of dose conversion coefficients for an eight-year-old Iranian male phantom undergoing computed tomography. Radiat Environ Biophys 2015;54:465-74.
29. United Nation Scientific Committee on the Effects of Atomic Radiation (UNSCEAR). Sources and Effects of Ionizing Radiation, Report to the General Assembly with Scientific Annexes. Report Vol. I and II. United Nation Publication. New York; 2008. p. 1-776.
30. Moore WH, Bonvento M, Olivieri-Fitt R. Comparison of MDCT radiation dose: A phantom study. AJR Am J Roentgenol 2006;187:W498-502.
31. Berrington de González A, Mahesh M, Kim KP, Bhargavan M, Lewis R, Mettler F, *et al*. Projected cancer risks from computed tomographic scans performed in the United States in 2007. Arch Intern Med 2009;169:2071-7.
32. Paterson A, Frush DP. Dose reduction in paediatric MDCT: General principles. Clin Radiol 2007;62:507-17.
33. McCollough CH, Bruesewitz MR, Kofler JM Jr. CT dose reduction and dose management tools: Overview of available options. Radiographics 2006;26:503-12.
34. The American Association of Physicists in Medicine (AAPM). AAPM Position Statement on the Use of Bismuth Shielding for the Purpose of Dose Reduction in CT Scanning. Available from: https://www.aapm.org/publicgeneral/BismuthShielding.pdf. [Last accessed on 2016 May 07].
35. Aichinger H, Dierker J, Joite-BarfuB S, Sabel M. Radiation Exposure and Image Quality in X-ray Diagnostic Radiology. 1st ed. Berlin, Heidelberg: Springer; 2004.
36. Foley SJ, McEntee MF, Rainford LA. An evaluation of in-plane shields during thoracic CT. Radiat Prot Dosimetry 2013;155:439-50.
37. International Commission on Radiological Protection (ICRP). Radiological protection in paediatric diagnostic and interventional radiology. In: Khong PL, Ringertz H, Donoghue V, Frush D, Rehani M, Appelgate K, *et al*. editors. ICRP publication 121. Ann ICRP 2013;42:1-63.
38. Akhlaghi P, Miri Hakimabad H, Rafat Motavalli L. Dose estimation in reference and non-reference pediatric patients undergoing computed tomography examinations: A Monte Carlo study. Radioprotection 2015;50:43-54.